Near-Complete Absorption of Intense, Ultrashort Laser Light by Sub-λ Gratings

Subhendu Kahaly,[1] S. K. Yadav,[2] W. M. Wang,[3] S. Sengupta,[2] Z. M. Sheng,[3,4]
A. Das,[2] P. K. Kaw,[2] and G. Ravindra Kumar[1]

[1]*Tata Institute of Fundamental Research, 1 Homi Bhabha Road, Mumbai 400005, India*
[2]*Institute for Plasma Research, Bhat, Gandhinagar 382428, India*
[3]*Beijing National Laboratory of Condensed Matter Physics, Institute of Physics, CAS, Beijing 100190, China*
[4]*Department of Physics, Shanghai Jiao Tong University, Shanghai 200240, China*
(Received 18 January 2008; published 29 September 2008)

We demonstrate near-100% light absorption and increased x-ray emission from dense plasmas created on solid surfaces with a periodic sub-λ structure. The efficacy of the structure-induced surface plasmon resonance, responsible for enhanced absorption, is directly tested at the highest intensities to date (3×10^{15} W cm^{-2}) via systematic, correlated measurements of absorption and x-ray emission. An analytical grating model as well as 2D particle-in-cell simulations conclusively explain our observations. Our study offers a definite, quantitative way forward for optimizing and understanding the absorption process.

The interaction of intense, ultrashort laser pulses with optically flat solid surfaces results in hot solid density plasmas which, on the one hand, display exotic physics [1] and, on the other, offer fascinating applications in laser fusion [2], novel x-ray sources, particle acceleration, and medical therapies [1,3]. The crucial aspect that facilitates all of these is the generation and transport of fast electrons. It is well known that fast electrons arise out of high intensity laser absorption in collisionless plasmas. There has been a tremendous effort to enhance hot electron generation via improved laser coupling to the plasma. Attempts to create preplasma for further excitation by intense laser pulses have been successful [4], but major improvements have resulted from "structuring" the target surface with nanoparticles [5], nanowires [6], and other such deposits [7–9]. Ideally, such modulations are best studied when they are "controllable," viz., periodic structures. Some early work with grating targets has shown attractive enhancement of hot electron generation which has been qualitatively attributed to the surface plasmons excited in such structures [7,8,10]. However, there has been no clear, quantitative link established among enhanced absorption, surface plasmon resonance, and increased hot electron generation—more importantly, under actual conditions relevant for solid density hot plasma generation.

In this Letter, we demonstrate near-100% absorption of intense, femtosecond laser pulses by sub-λ grating targets at intensities relevant to both scientific and technological perspectives. We present a complete, systematic, and correlated study of controlled enhancement of absorption and hot electron generation on grating surfaces. Specifically, we establish the role of surface plasmons at the highest intensity levels ever (3×10^{15} W cm^{-2}) in surface structures under well-defined experimental conditions. We present these results against the backdrop of polished gold surfaces. We then adopt two ways to explain the

results: (1) an analytical model based on the formalism of Chandezon *et al.* [11], with appropriate numerics, and (2) 2D particle-in-cell (PIC) simulations that for the first time use a modulated plasma front. This is the first time that data under high intensity conditions have been modeled both analytically and with PIC simulations. We obtain clear agreement with both, thus benchmarking the theory with experiment.

In our experiments a Ti:sapphire chirped pulse amplified laser (55 fs, 800 nm, 10 Hz) is focused to 60 μm (peak intensity 4×10^{15} W cm^{-2}) with an $f/20$ lens on targets in a vacuum chamber (10^{-5} torr). The beam is focused loosely so as to have a well-defined angle of incidence by minimizing beam divergence. The target is constantly translated in the focal plane to expose a fresh surface to each laser pulse. The nanosecond prepulse level is 5×10^{-6} and does not cause any significant preplasma at the highest intensity. Basic characterization experiments use a continuous wave laser and an unamplified nanojoule, 55 fs mode-locked pulse train (74 MHz) from the same laser system. Reflected laser pulses are collected using calibrated photodetectors. Hard x-ray bremsstrahlung (25–250 keV) under high intensity laser irradiation is measured using NaI(Tl) scintillating detectors. We used two types of targets—(a) triangular blazed gratings with Au coating on a glass substrate (Jobin Yvon) and (b) polished ($\lambda/10$) Au coated glass targets. The thickness of the gold layer in both cases is many times the optical skin depth, $\delta_s \sim c/\omega_p \approx 0.022$ μm in our case, so that the glass background does not have any significant role to play. The grating wave vector is aligned in the plane of incidence (Fig. 1, inset).

A sub-λ ($\lambda/d < 1$) grating permits only two diffraction orders, i.e., the specularly reflected one $m = 0$ and the $m = -1$th order [12]. Low intensity p-polarized light shows a sharp dip in specular reflectivity (Fig. 1) with the minimum at an angle $\theta_{sp} = 23°$. At this angle, most of the light ($\sim 84\%$) that is incident is completely absorbed.
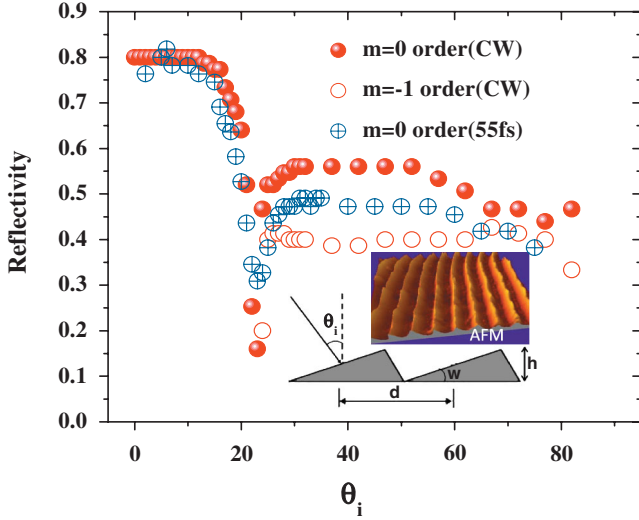
FIG. 1 (color).   Sub-λ grating diffraction; θ_i incident angle. Inset: Atomic force microscope (AFM) image of the grating (period, **d** = 555 nm; groove depth, **h** = 158 nm; blaze angle, **w** = 17.45°).

FIG. 2 (color).   Gold reflectivity vs light intensity for *s* and *p* polarizations, $\theta_i = 23°$. The knees here and in Fig. 3 correspond to plasma formation thresholds I_{Th}.

For *p* polarization, θ_{sp} is the angle at which the phase-matching condition is satisfied and the surface plasmon resonance (SPR) is activated. Please note the angular sharpness of the resonance for the low intensity femtosecond laser pulse, in spite of its large bandwidth (50 nm). We made a comparative study of the reflectivity of *p*- and *s*-polarized light from gratings (Fig. 3) and optically flat Au surfaces (Fig. 2) at $\theta_i = \theta_{sp} = 23°$, while varying the intensity of incident light over 3 orders of magnitude. This measurement is important to see the onset of plasma formation in both cases and to study the excitation of surface plasmons at high intensities, an aspect not addressed until now. We see that the flat Au target displays metallic reflectivity until $I_{Th} \sim 4.5 \times 10^{13}$ W cm^{-2}, the plasma formation threshold (PFT) for the material. Beyond this value, plasma is formed at the leading edge of the laser pulse, and the rest of the light is reflected from the gold plasma which reflects less than the gold metal. One may note that there is not much difference between the *p* and *s* polarizations. With the grating target, the reflectivity (note that there is only one diffraction order for $\theta_i = \theta_{sp}$) for *s* polarization shows exactly the same behavior as optically flat Au with the same PFT. The reflectivity of *p*-polarized light from the grating target, on the other hand, shows interesting differences. At low intensity, it starts from the value 0.33, which, as expected, matches the reflectivity of ultrashort pulse with SPR (Fig. 1). The PFT is also dramatically reduced by a factor of 3 to a value $I_{Th} \sim 1.5 \times 10^{13}$ W cm^{-2}. Further, the absorption of *p*-polarized light increases with increasing intensity and at about 2×10^{15} W cm^{-2} reflectivity drops by 4.7 times its low intensity value and almost 93% of the incident light is absorbed. The drop in the PFT intensity for the *p*-polarized case can be explained by assuming that the amount of energy absorbed at the
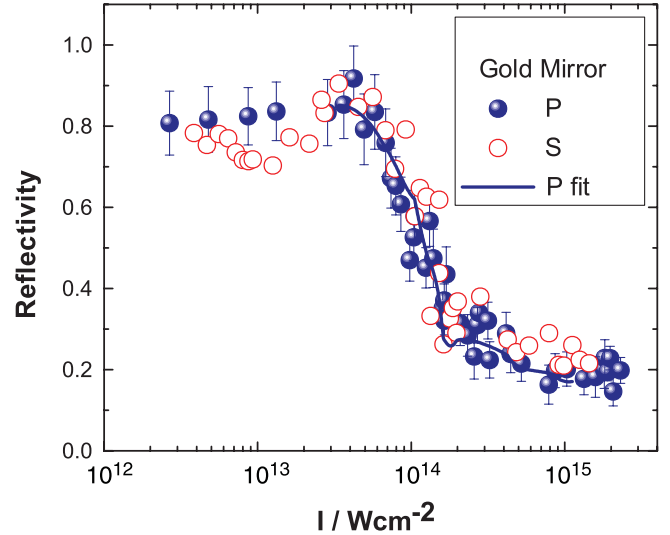
threshold point is the same for both the grating target (*G*) and the plain mirror target (*M*), i.e., $f_G . I_{Th,G} \approx f_M . I_{Th,M}$, where f is the fractional absorption and I_{Th} is the threshold intensity. Taking the measured values $f_G \approx 0.67$, $f_M \approx 0.17$, and $I_{Th,M} \approx 4.5 \times 10^{13}$ W cm^{-2}, we get $I_{Th,G} \approx 1.14 \times 10^{13}$ W cm^{-2}, which matches closely with the observed PFT intensity for the grating target.

The reflectivity of *s*- and *p*-polarized light at the fixed angle of incidence ($\theta_i \sim 23°$) as a function of laser intensity for a plane Au target (Fig. 2) can be understood by studying the propagation of a plane electromagnetic wave through an inhomogeneous, short scale length ($L/\lambda < 1$) plasma, whose permittivity is chosen to be that of a Drude metal, i.e., $\epsilon = 1 - \omega_p^2/\omega(\omega + i\nu)$ [13,14]. Here the col-
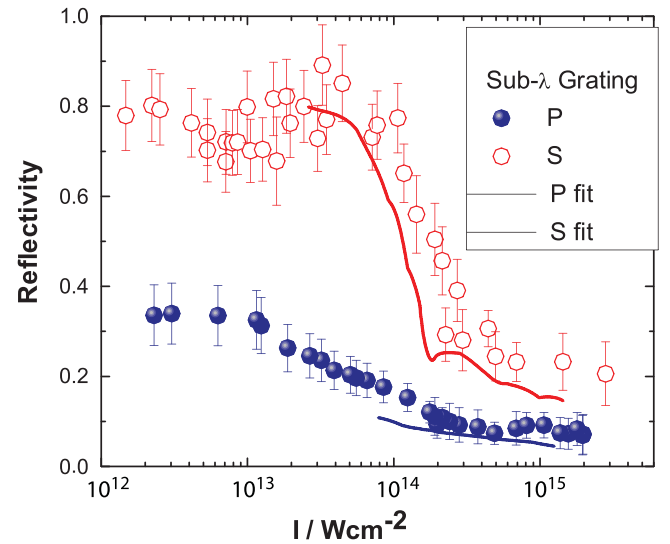

FIG. 3 (color).   Grating reflectivity vs light intensity for *s* and *p* polarizations, $\theta_i = 23°$.

lision frequency ν depends on laser intensity I through electron density and temperature (n_e and T_e) or through some polarization-independent nonlinear processes [15]. Using $T_e \sim 100$ eV at $I \sim 10^{15}$ W/cm^2 and $\nu_{\exp} = \frac{2}{\gamma-1} \times \sqrt{ZT_e/m_i}$ [13,16], we estimate the electron temperature at all intensities ($I_{abs} \propto n_e T_e \nu_{\exp}$), which in turn gives an estimate of density scale length $L \approx a\nu_{\exp}\tau$ ($a \sim 0.5$ [13]) at different laser intensities. Choosing an exponential density profile with density scale length (L/λ) and taking $\nu/\omega \propto n_e$ (following Ref. [13]), we calculate the effective collision frequency $(\nu/\omega)_{\text{eff}}$ at the solid surface by matching the calculated reflectivity and the measured reflectivity for s-polarized light. We further use this effective collision frequency and the independently evaluated L/λ to calculate the reflectivity of p-polarized light as a function of laser intensity [13]. The solid line in Fig. 2 shows the calculated reflectivity of p-polarized light from the plane Au target beyond I_{Th} ($\sim 4.5 \times 10^{13}$ W/cm^2); it matches closely with the measured data. We further note that our results are independent of the chosen density profile [16].

We now use the information obtained above [dependence of $(\nu/\omega)_{\text{eff}}$ on the laser intensity I] to explain the grating results. For our laser parameters ($I \sim 10^{15}$ W/cm^2 and $\tau_{\text{pulse}} \sim 55$ fs), $L/\lambda \sim 10^{-3}$ at the highest intensity, implying that the short scale length plasma formed at the grating surface retains the imprint of the grating structure during the entire interaction time. This allows us to use the formalism suggested by Chandezon *et al.* [11,17] to explain the reflectivity of both s- and p-polarized light as a function of laser intensity for the grating target (Fig. 3). It uses a generalized coordinate system which maps the structured grating surfaces to planar surfaces. In the formalism (a) it makes the matching of boundary conditions easy and (b) it also allows transformation of Maxwell's equations in Fourier space into a matrix eigenvalue problem making the numerical solution of the grating problem straightforward. The inputs needed for this calculation are the grating parameters, which are known, and the dielectric constant as a function of laser intensity. Assuming Drude permittivity as before, and the above calculated values of $(\nu/\omega)_{\text{eff}}$ at the solid surface as a function of laser intensity, we calculate the dielectric constants at different intensities. We note here that, for the same p-polarized input laser intensity, the actual electric field seen by the grating target is enhanced in SPR. This effect is incorporated by selecting $(\nu/\omega)_{\text{eff}}$ corresponding to enhanced intensities after taking an appropriate average enhancement factor. These are then used to calculate the grating reflectivity at different intensities. The solid lines in Fig. 3 show the results of our calculation. The close match with experiments is a clear vindication of the Chandezon formalism. Thus we see that, with only one experimental input, i.e., s reflectivity as a function of intensity, all of the other results are derivable from analytical or numerical calculations.

The absorbed light generates hot electrons in the plasma which give rise to hard x-ray bremsstrahlung. The x-ray spectrum from high intensity laser-produced plasma on a flat gold-coated glass target shows hot electrons of only one temperature, though p polarization ($T_h = 15 \pm 0.7$ keV) produces hotter electrons than s polarization ($T_h = 11.8 \pm 0.4$ keV). Figure 4(a) shows hard x-ray spectrum from the grating plasma at $I = 3.8 \times 10^{15}$ W cm^{-2} when the laser is incident at $\theta_i = \theta_{sp}$. s polarization gives rise to a Maxwellian spectrum with $T_h = 16 \pm 1$ keV, while for p polarization the spectrum shows a non-Maxwellian distribution with two temperatures: $T_{h1} = 14 \pm 3$ keV and $T_{h2} = 67 \pm 11$ keV. The higher component constituting 14% of the total counts is due to collisionless damping of surface plasmons. The hard x-ray yield for p-polarized light is 4.8 times that of the s-polarized case. The crucial role of SP coupling in the enhanced generation of hotter electrons from the grating plasma is verified by looking at the hard x-ray spectrum at a non-SPR ($\theta_{sp} \neq \theta_i = 45°$) angle of incidence [Fig. 4(b)]. Here, s polarization produces one temperature electron distribution at $T_h = 8.7 \pm 0.2$ keV. p polarization gives rise to mainly (99% weightage) one hot electron temperature at $T_h = 9 \pm 1$ keV and a very feeble high temperature component around 26 ± 11 keV.

To explain these experimental results, we have conducted 2D PIC simulations on laser interaction with grating targets [18]. We have taken the laser pulse with a duration of 20 laser cycles and normalized amplitude $a_0 = 0.05$, corresponding to a laser intensity of 3.4×10^{15} W/cm^2, which is close to the experimental conditions. The initial density of the target plasma is $25n_c$. We take a thin target of 2 μm without preplasma. The triangular grating is strictly identical in the geometric shape to that adopted in the experiments. The p reflectivity as a function of incident angles is shown in Fig. 5(a). It shows that there is an absorption peak (reflection depression)
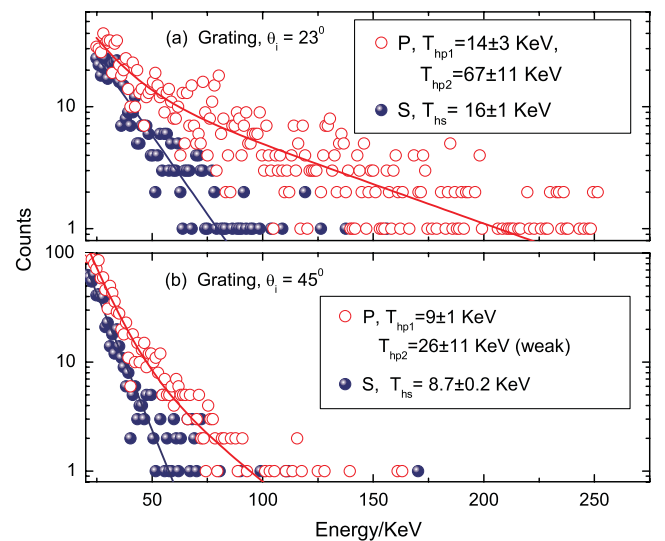

FIG. 4 (color). Bremsstrahlung spectra for the grating plasma at intensity $I = 3.8 \times 10^{15}$ W cm^{-2} with (a) $\theta_i = 23°$ and (b) $\theta_i = 45°$. Solid curves denote least squares temperature fits.
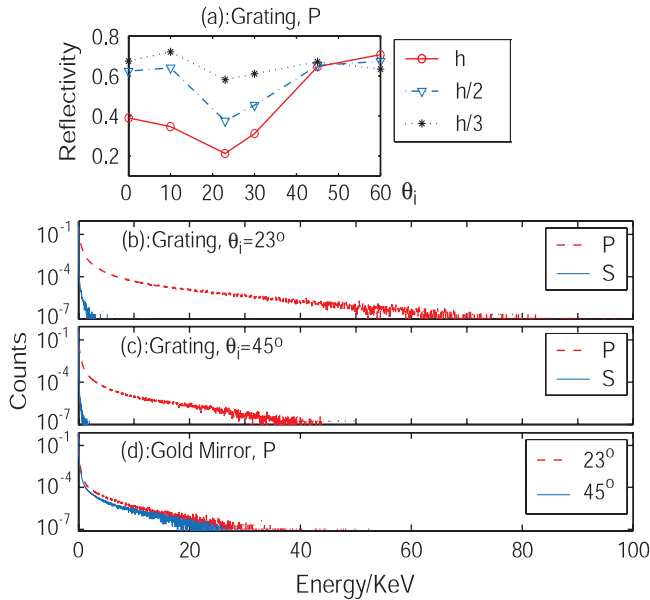
FIG. 5 (color). (a) Reflectivity as a function of angle of inci-
dence from PIC simulation for the grating plasma with different
groove depths h, $h/2$, and $h/3$, where $h = 158$ nm taken from
the experiment. Electron energy distribution at the exit of laser
pulse at (b) $\theta_i = 23°$ and (c) $\theta_i = 45°$ for the grating (groove
depth h) plasma and for the flat gold target (d).

around $\theta_i = 23°$, which is around the same angle as ob-
served in low intensity experiments (Fig. 1). As one re-
duces to $1/2$ or $1/3$ of the original groove depth, the
reflection is increased and the plasmon resonance (around
$23°$) tends to disappear. Figures 5(b) and 5(c) plot the
electron energy distributions obtained at the time when
the incident laser just leaves the target surface. The higher
component of the hot electron temperature for p-polarized
light calculated from the electron energy distribution for
$\theta_i = 23°$ turns out to be ~ 51.9 keV, which is close to
67 ± 11 keV measured in experiments. At $\theta_i = 45°$
[Fig. 5(c)], similar to experiments, a very weak higher
component of hot electron temperature ~ 37.5 keV is
seen. The low temperature component with p-polarized
light, in both of the above cases, as well as the hot electron
temperature produced by s-polarized light do not match the
experimental results. This can be due to the fact that the
low temperature component is mainly produced via colli-
sional mechanisms not included in the PIC simulations,
whereas the high temperature component which is pro-
duced via collisionless absorption mechanism (SPR) is
well-modeled by PIC simulation. Further, the hot electron
temperature with p-polarized light observed for the grating
target is significantly higher than that observed for the
planar target as can be seen from Fig. 5(d). Thus PIC
simulation qualitatively reproduces the experimental
observations.

Thus we see that it is possible to enhance light coupling
to near-100% levels in the high intensity regime by ex-
ploiting SPR. The very short length scale plasma retains
the imprint of grating structure in its profile during its
interaction with the incident pulse. The reflectivity curves
show that the high level of light absorption is maintained
even when we increase the light intensity over 3 orders of
magnitudes. The lowering of the threshold of plasma for-
mation in grating targets is because of the fact that rela-
tively more light is absorbed under conditions favorable to
SPR. This presents a very attractive opportunity for tuning
the absorption (by varying incident angles and/or polar-
izations) and hence controlling the flux and energies of hot
electrons and x rays from laser-produced, solid plasmas.
The intensities we have examined are easily available from
multikilohertz repetition rate, femtosecond lasers, and this
should spur a great deal of progress in designing x-ray
sources from grating targets.

In conclusion, we have studied the reflectivity of a 1D
sub-λ periodic Au structure as a function of light intensity,
over 3 orders of magnitude, at an angle of incidence that
maintains SPR at low intensity. We see almost complete
absorption of light. From the bremsstrahlung at high inten-
sity, we observe that SPR is assisting the generation of
hotter electrons in larger numbers. One can tune the hot
electron temperature by switching the polarization state of
the light and choosing the angle of incidence very pre-
cisely. Our observations are completely backed by an
analytical model as well as PIC simulations. Our study
provides direct evidence that surface plasmons enable
efficient coupling of light and plasmas at intensities prev-
alent in intense laser-solid interaction studies.

[1] G. A. Mourou *et al.*, Rev. Mod. Phys. **78**, 309 (2006).
[2] M. Tabak *et al.*, Phys. Plasmas **1**, 1626 (1994).
[3] V. Malka *et al.*, Rev. Sci. Instrum. **77**, 03B302 (2006).
[4] See, e.g., C. Gahn *et al.*, Appl. Phys. Lett. **73**, 3662 (1998).
[5] P. P. Rajeev *et al.*, Phys. Rev. Lett. **90**, 115002 (2003).
[6] G. Kulcsar *et al.*, Phys. Rev. Lett. **84**, 5149 (2000).
[7] S. P. Gordon *et al.*, Opt. Lett. **19**, 484 (1994).
[8] M. M. Murnane *et al.*, Appl. Phys. Lett. **62**, 1068 (1993).
[9] A. L. Lei *et al.*, Phys. Rev. Lett. **96**, 255006 (2006).
[10] J. C. Gauthier *et al.*, Proc. SPIE Int. Soc. Opt. Eng. **2523**, 242 (1995).
[11] J. Chandezon *et al.*, J. Opt. Soc. Am. **72**, 839 (1982).
[12] M. C. Hutley *et al.*, Opt. Commun. **19**, 431 (1976).
[13] H. M. Milchberg *et al.*, J. Opt. Soc. Am. B **6**, 1351 (1989).
[14] H. M. Milchberg *et al.*, Phys. Rev. Lett. **61**, 2364 (1988).
[15] P. Kaw *et al.*, Phys. Rev. Lett. **25**, 430 (1970).
[16] M. K. Grimes *et al.*, Phys. Rev. Lett. **82**, 4010 (1999).
[17] L. Li *et al.*, J. Opt. Soc. Am. A **13**, 2247 (1996).
[18] Z.-M. Sheng *et al.*, Phys. Rev. E **69**, 025401(R) (2004).